Microemulsion based synthesis of inorganic barium sulphate nanoparticles using various cosurfactants

M. MOOSA[a], M. IKRAM[b], S. ALI[a,b], ISLAH-U-DIN[a]

[a]*Materials and Nanoscience Research Lab (MNRL), Department of Physics, Government College University, Lahore, 54000, Punjab, Pakistan*
[b]*Solar Applications Research Lab, Department of Physics, Government College University, Lahore, 54000, Punjab, Pakistan*

Inorganic nanoparticles (NPs) of barium sulphate ($BaSO_4$) were synthesized using the microemulsion route with various cosurfactants. Polyethylene glycol (PEG) was used along with cosurfactants methanol, propanol and hexanol to improve the solubility of polar compounds in non-polar compounds. The addition of alcohols from long carbon chain to small carbon chain increased the rate of intermicillar exchange and decreased the particle size. X-Ray diffraction (XRD) confirms the crystallite size range around 15-20 nm spherical morphology of the particles was observed using Scanning Electron Microscopy (SEM). The symmetrical vibration of SO_4^{-2} was confirmed by Fourier Transform Infrared (FTIR) at 1079 cm^{-1} and it stays same for all cosurfactants. Absorption was between 200-400 nm with a large band gap as confirmed by Ultraviolet-Visible (UV-Vis) Spectroscopy.

1. Introduction

The accuracy to generate self-assembled nanomaterials with controlled size stimulates both the surface chemists and the nanoscience engineers. The pragmatic approach to assemble small size materials formerly requires a kind of template for their synthesis [1]. Surfactants or amphiphiles play a vital role in this regard with their polar head (hydrophilic) and non-polar tail (lipophilic) adsorbing at the surfaces and interfaces of two immiscible liquids to reduce the surface tension and thus developing aggregates inside the solution to initiate microemulsions [2].

Sometimes, in the presence of surfactant, the process of solubilization slows down because of the poor solvent quality of water for non-polar compounds or due to high molecular weight of polymers. This situation can be substantially recovered by adding cosurfactants (alcohols) with surfactant [3–7].

The addition of alcohol molecules leads to arranged surfactant tails, thereby reducing tail–tail and micelle–micelle interactions as shown in Fig. 1 [8–10] or acts at the interface to reduce the surface stress [11,12]. By altering the solvent properties the aggregation of the primary surfactants can be achieved which leads to the formation of NPs [13]. Mostly used examples of cosurfactants are medium chain alcohols with 5–8 carbon units. A more detailed list of various surfactants can be found in a review by Lopez Quintala et al. [14].
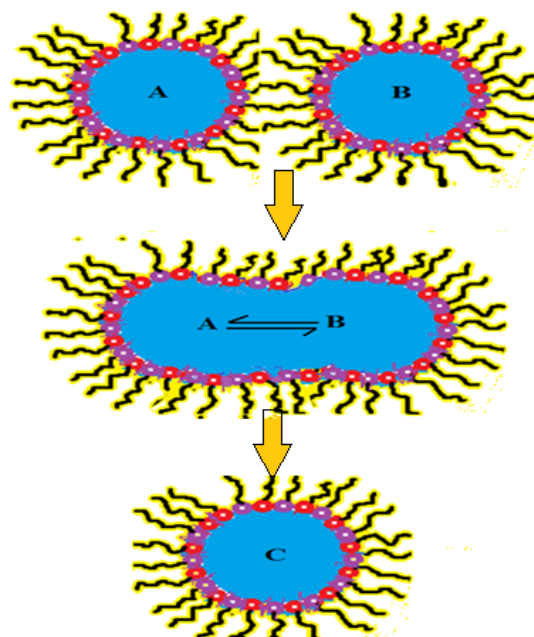

Fig. 1. The intermicillar exchange of ionic compounds during microemulsion. Surfactant molecules arrange themselves such that the tails are at the oil phase and heads attach to each other in order to trap water and form NPs.

Other than solubility, the effect of adding cosurfactants (intermediate chain length alcohols) on the size of particles has also been studied [15]. Bagawe and Khilar [16] studied the effect of varying carbon chain length of cosurfactants during reverse micelle synthesis of silver NPs and found a decrease in the particle size when

short chain length cosurfactant was used. Similarly, T.Charinpanitkul *et al.* reported cosurfactants with larger molecular size such as n-hexanol could provide a higher aspect ratio to synthesize ZnS nanoparticles than any other cosurfactant [17]. The effect on the particle size by varying cosurfactant from hexanol to methanol keeping non- ionic surfactant constant has also been observed. Studies revealed that the replacement of extended carbon chain alcohols with short carbon chain alcohols leads to a decrement in the particle size. The reason is the rate of inter- micellar exchange of reactants to form nanoparticles becomes slow which often leads to polydispersity.

To further explore the role of cosurfactants on the size and morphology of resulting nanostructures, inorganic $BaSO_4$ NPs, commonly referred as barite, were synthesized using various cosurfactants such as methanol, propanol and n-hexanol. Polyethylene glycol (PEG) was used as a non-ionic surfactant because of its low toxicity, ignorable ionization in aqueous solution and easy availability at large scale [18].
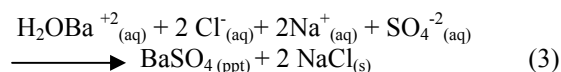
2. Experimental

2.1. Materials

The raw materials used as reactant species were ($BaCl_2$, Na_2SO_4), non-ionic surfactant polyethylene glycol (PEG) ($C_{2n}H_{4n+2}O_{n+1}$), with various cosurfactants methanol (CH_3OH), propanol ($CH_3CH_2CH_2OH$) and hexanol ($CH_3(CH_2)_5OH$). Kerosene ($C_{12}H_{26}$) was used to develop an oil phase and distilled water was used as solvent. Ethanol (CH_3CH_2OH) and acetone (C_3H_6O) were used for washing purposes.

2.2. Fabrication

The NPs of $BaSO_4$ were synthesized by simple precipitation reaction. The reaction steps in the process are given

$$H_2OBaCl_{2.(s)} \longrightarrow Ba^{+2}_{(aq)} + 2\ Cl^-_{(aq)} \quad (1)$$

$$H_2ONa_2SO_{4\ (.s)} \longrightarrow 2Na^+_{(aq)} + SO._4^{-2}_{(aq)} \quad (2)$$

$$H_2OBa^{+2}_{(aq)} + 2\ Cl^-_{(aq)} + 2Na^+_{(aq)} + SO_4^{-2}_{(aq)}$$
$$\longrightarrow BaSO_{4\ (ppt)} + 2\ NaCl_{(s)} \quad (3)$$

Reaction solutions were prepared by adding 0.5 M of $BaCl_2$ and 0.5 M of Na_2SO_4 in 20 ml distilled water. To prepare water in oil (W/O) microemulsion, 10 ml of non-ionic surfactant -PEG dissolved in 40 ml of kerosene (Fig. 2). Three samples were prepared by adding cosurfactants methanol, propanol, or hexanol in the blend of PEG + kerosene. The molar ratio of cosurfactant and non-ionic surfactants was kept 4:1 and the solution turned transparent after stirring.

The prepared salt solution was added dropwise to this surfactant blend under vigorous[9] stirring for 30 mins at 190 rpm. The system was kept stable afterwards for complete[5] precipitation. Afterwards, the solution was filtered with a filter paper to collect the precipitates and washed alternately with acetone and ethanol[11] for several times. The final product was dried in hot air oven`for 6 hours at 100 °C. The flow chart is shown in Fig. 2.
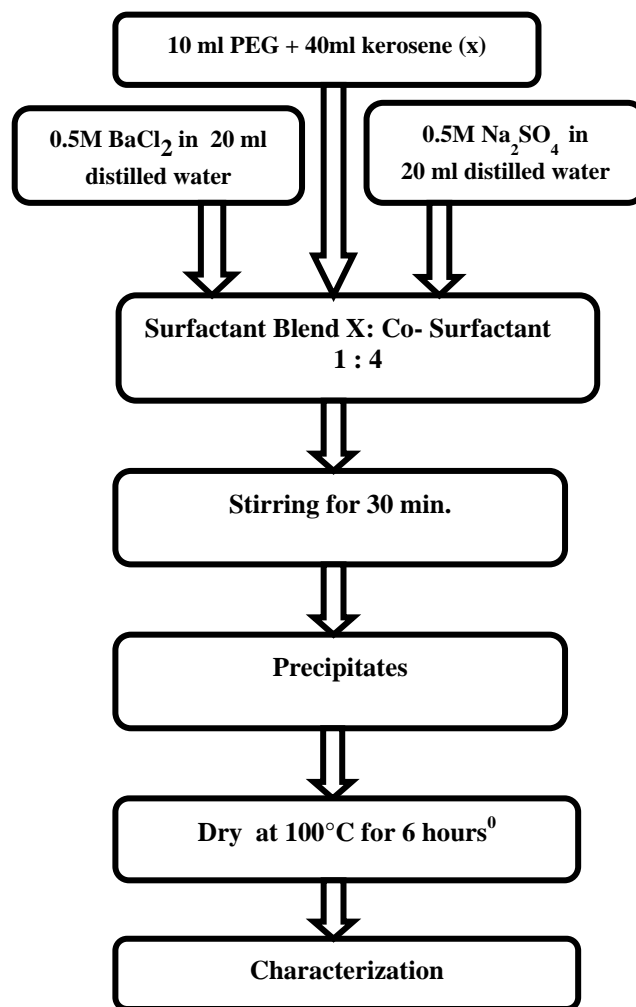

Fig. 2. Flow sheet representing the experimental procedure

2.3. Characterization

The XRD measurements were performed using X'PERT PRO PAN analytical diffractometer with a source[$] of CuKα ($\lambda$=1.5419 A[0]), voltage 40 kV, and a current 40 mA. During diffractogram measurement`, a narrow slit` of 1.52 mm was used. The diffraction patterns were obtained in the region $20° \leq 2\theta \leq 80°$. Ultra Large VP-SEM model S-3700N Hitachi, Japan was used to analyze the morphology of $BaSO_4$ NPs. Perkin Elmer[$@] R-X1spectrophotometer was used to record the IR- spectra of the sample and the absorption spectra were recorded using GENESYS 10S UV-VIS spectrophotometer.

3. Results and discussion

The XRD patterns of BaSO$_4$ NPs synthesized by PEG + methanol **(a)** PEG + propanol **(b)** and PEG + n-hexanol **(c)** are shown in Fig. 3. The diffraction peaks of BaSO$_4$ were fully matched with JCPDS [00-001-1229]. Broadened peaks from sample **c** confirm smaller crystallite size of the materials. This broadening can be attributed to the use of long chain cosurfactant (hexanol) in synthesis of **c** as compared to small carbon chain cosurfactant (methanol) for **a.** As a result solubilization of two immiscible liquids improved, causing the rate of intermicillar exchange to slow down resulting in large polydisperse products that demonstrate poor crystallinity and hence broader diffraction peaks. The crystallite sizes were found to be 16, 18 and 19 nm for samples **a**, **b** and **c** respectively using the Scherrer equation.
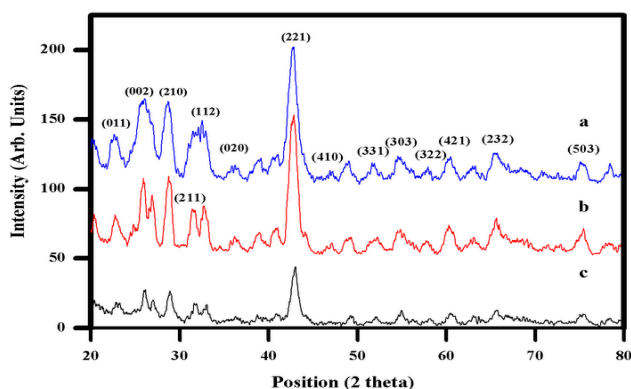

Fig. 3. X-ray diffractogramsof BaSO$_4$ -NPs using (a) PEG+ methanol , (b) PEG + propanol &(c) PEG + hexanol

SEM images of prepared samples are shown in Fig. 4 (a-c). The images portray clusters of spherical shaped BaSO$_4$ NPs distributed uniformly. The rate of agglomeration varied due to the presence of ethoxide group on the surface of particles that acted as a shell against flocculation [19,20]. Moreover, PEG with diverse cosurfactants replaced the coordinated water and reduced the surface$^\$$ tension effectively when moved from small carbon chain alcohol to long carbon chain alcohol leading to a slight change in the particle sizes. Furthermore, the small carbon chain cosurfactants not only decreased the number of free steps involved in the reaction, but also inhibited the growth process of particles resulting in final product with high dispersity and small particle size [21]. On the other hand, hexanol that was distributed over the particles'$^{7.5}$surface lead PEG at the sub-phase to enhanced binding of barium ions at the interface that directed to large particle size. According to Limin Qi *et al.* (1996), cubic shaped BaSO$_4$ NPs can be obtained if the water content is maximum [18] but in the present study spherical NPs were achieved which shows that less water content was involved.
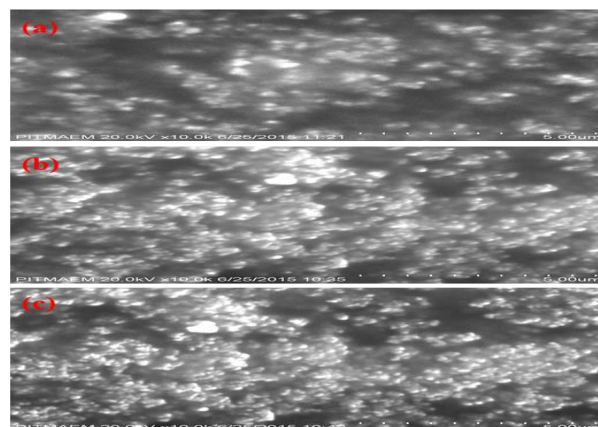

Fig. 4. SEM images of BaSO$_4$ -NPs: (a) PEG + methanol, (b) PEG + propanol and (c) PEG + hexanol.

FTIR results of all samples are shown in Fig. 5. It can be seen that all the transmittance peaks appeared at the same frequencies irrespective of the choice of cosurfactants. Absence of any significant peak shift can be attributed to presence of identical functional groups in all samples.
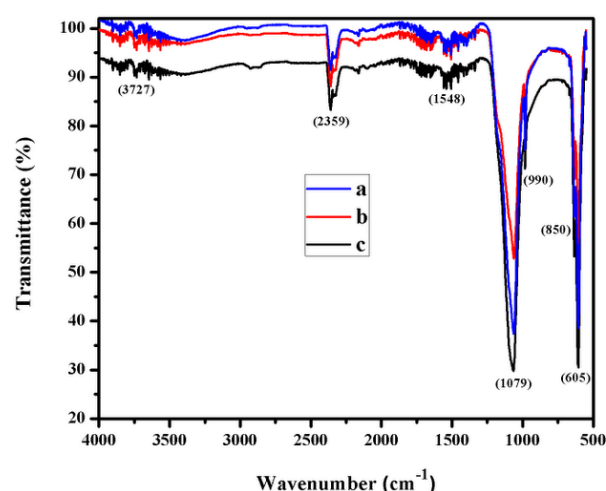

Fig. 5. Interferogram of BaSO$_4$ NPs: a) PEG +methanol, b) PEG + propanol & c) PEG + hexanol.

Dominant vibrational modes appear at wavenumbers 3727, 2359, 1548, 1079, 990, and 605 cm^{-1}. The sulfur-oxygen (S-O) stretching was usually identified in the region 1083- 1179 cm^{-1} [22] confirmed that the bands axial in the spectrum (Fig. 4) at 1079 cm^{-1} with shoulder at 990 cm^{-1} was due to the symmetrical vibration of SO$_4^{-2}$. The peak at 605cm^{-1} is attributed to SO$_4^{-2}$ out-of-plane bending vibration [23]. Generally, bending bands are shaper than the stretching bands which can be seen in the spectrum. Bands derived from carbon dioxide appear at 2359 cm^{-1} was due to its 1% presence in the air [24,25]. Similarly, the peak at 1548 cm^{-1} was usually due to the presence of alkyl substitution that specified the presence of polyether. Finally, the vibrational modes at about 3727 cm$^{-1`}$ are attributed to the stretching and deformation of hydroxyle groups.

UV-Vis spectroscopy measurements of all three samples are shown in Fig. 6. It can be observed that by varying cosurfactants from methanol to hexanol no peak shifting takes place which signified surfactant blend imparted no significant changes to the chemical structure of the $BaSO_4$ NPs. The absorbance of various cosurfactant based samples centered around 320 nm with minute blue shifts for samples containing larger carbon chains.
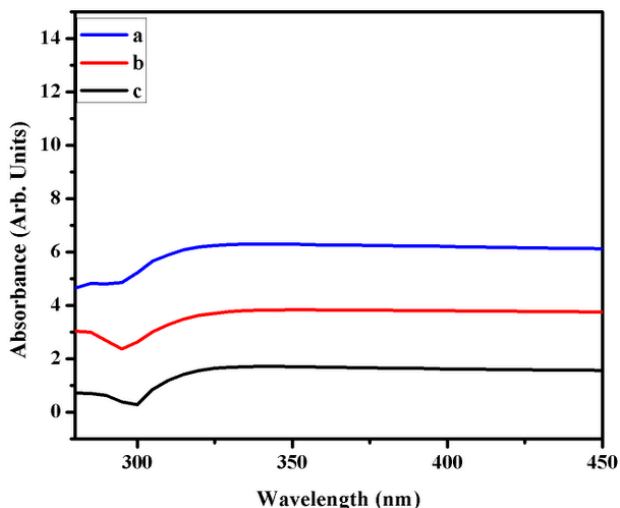

Fig. 6. The absorption spectra of $BaSO_4$- NPs with
a) PEG + methanol , b) PEG+ propanol and
c) PEG + hexanol.

Band gap energies were calculated using linear plots of $(\alpha\ h\ \nu)^{1/r}$ against (h ν) for all the samples as shown in Fig. 6. It can be seen that decreasing carbon chain length of cosurfactants for $BaSO_4$ - NPs lead to an increase in the optical band gap. A decrease in the energy band gap with increasing carbon chain can attributed to increase structural disorder.
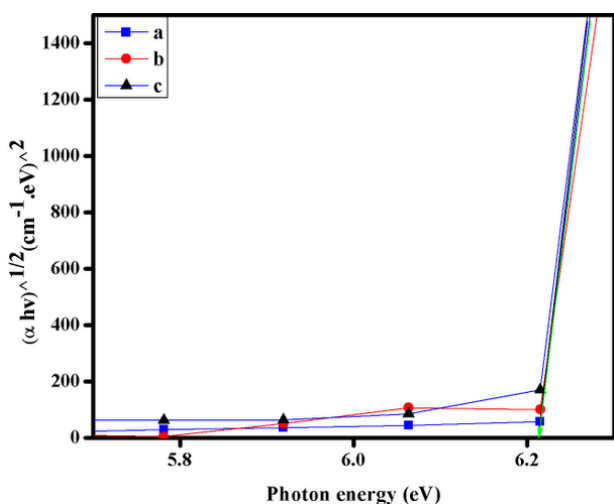

Fig. 7. Band gap of $BaSO_4$ _NPs with (a) PEG + methanol,
(b) PEG + propanol and (c) PEG + hexanol

4. Conclusion

In summary, $BaSO_4$ NPs with controlled size were synthesized using various cosurfactants while keeping PEG constant. It is evident from XRD that grain size decreases upon varying cosurfactants from hexanol to methanol. The decrease in the grain size is attributed to slower rate of intermicillar exchange during growth of nanoparticles. The SEM images show clusters of spherical $BaSO_4$ NPs with small and large agglomeration due to presence of water in the samples. Vibrational modes of all the samples were observed at the identical   frequencies with no peak shifting which can be attributed to similar functional groups involved in all samples of $BaSO_4$. Maximum absorbance of $BaSO_4$NPs was centered around 320 nm as observed from UV-Vis spectroscopy. The band gap of for all three samples are 5.17 eV, 5.16 eV and 5.16 eV as calculated from Tauc plot. The slight decrease in the band gap energies can be attributed to structural disorder caused by different cosurfactants.

References

[1] J. Stauff, Solvent Properties of Amphiphilic Compounds, von P. A. Winsor. Butterworths Scientific Publ. Ltd., London. 1954. 1. Aufl. IX, 270 S., gebd. 40 s, Angew. Chemie. **68**, 504 (1956).
[2] L.M. Liz-Marzán, P. V. Kamat, eds., Nanoscale Materials, Kluwer Academic Publishers, Boston, 2004. doi:10.1007/b101855.
[3] J. Liu, B. Han, G. Li, Z. Liu, J. He, G. Yang, Fluid Phase Equilib. **187-188,** 247 (2001).
[4] J. Liu, B. Han, J. Zhang, T. Mu, G. Li, W. Wu, et al., Fluid Phase Equilib. **211,** 265 (2003).
[5] G.J. McFann, Ph.D. Thesis, The University of Texas, (1993). http://repositories.lib.utexas.edu/bitstream/ handle/2152/2960/smithjrp98905.pdf
[6] G.J. McFann, K.P. Johnston, S.M. Howdle, AIChE J. **40**, 543 (1994).
[7] K. Sawada, T. Takagi, M. Ueda, Dye. Pigment. **60,** 129 (2004).
[8] V. Bansal, D. Shah, J. O'connell, J. Colloid Interface Sci. **75,** 462 (1980).
[9] M.J. Hou, D.O. Shah, Langmuir. **3,** 1086 (1987).
[10] D.J. Mitchell, B.W. Ninham, J. Chem. Soc. Faraday Trans. 2. **77,** 601 (1981).
[11] N. Asgharian, P. Otken, C. Sunwoo, W.H. Wade, Langmuir. **7,** 2904 (1991).
[12] P.G. De Gennes, C. Taupin, J. Phys. Chem. **86**, 2294 (1982).
[13] M. Kahlweit, R. Strey, G. Busse, J. Phys. Chem. **95.** 5344 (1991).

[14] M.A. López-Quintela, C. Tojo, M.C. Blanco, L. García Rio, J.R. Leis, Curr. Opin. Colloid Interface Sci. **9,** 264 (2004).

[15] V. Uskoković, M. Drofenik, Surf. Rev. Lett. **12,** 239 (2005).

[16] R.P. Bagwe, K.C. Khilar, Langmuir. **16,** 905 (2000).

[17] T. Charinpanitkul, A. Chanagul, J. Dutta, U. Rungsardthong, W. Tanthapanichakoon, Sci. Technol. Adv. Mater. **6,** 266 (2005).

[18] L. Qi, J. Ma, H. Cheng, Z. Zhao, Colloids Surfaces A Physicochem. Eng. Asp. **108,** 117 (1996).

[19] M.H. Talat, K.S. Jamil, The effect of surfactants on the particle size and optical properties of precipitated ZnO nanoparticles, (2009).

[20] Y. Nagasaki, Sci. Technol. Adv. Mater. **11**, 054505 (2010).

[21] P. Somasundaran, Encyclopedia of Surface and Colloid Science, Second Edition - Eight-Volume Set (Print) - CRC Press Book, **2**, 6186 (2006).

[22] P.F.K. H. H. Adler, Variations in infrared spectra, molecular symmetry and site symmetry of sulfate minerals, (1965) 132–147. http://www.minsocam.org/ammin/ am50/am50_132.pdf

[23] Y. Shen, C. Li, X. Zhu, A. Xie, L. Qiu, J. Zhu, J. Chem. Sci. **119,** 319 (2007).

[24] M. J. Baillie, D.H. Brown, K.C. Moss, D.W.A. Sharp, Anhydrous metal trifluoroacetates, J. Chem. Soc. A Inorganic, Phys. Theor. (1968) 3110.

[25] H. Eloussifi, J. Farjas, P. Roura, J. Camps, M. Dammak, S. Ricart, et al., Evolution of yttrium trifluoroacetate during thermal decomposition, J. Therm. Anal. Calorim. **108**, 589 (2011).

_____

[*]Corresponding author: mianraj.1981@gmail.com